ANTIMICROBIAL AGENTS AND CHEMOTHERAPY, May 2005, p. 1898–1906 Vol. 49, No. 5
0066-4804/05/$08.00+0 doi:10.1128/AAC.49.5.1898–1906.2005

Selective Intracellular Activation of a Novel Prodrug of the Human Immunodeficiency Virus Reverse Transcriptase Inhibitor Tenofovir Leads to Preferential Distribution and Accumulation in Lymphatic Tissue

William A. Lee,[1]* Gong-Xin He,[1] Eugene Eisenberg,[1] Tomas Cihlar,[1] Swami Swaminathan,[1] Andrew Mulato,[1] and Kenneth C. Cundy[2]

Gilead Sciences, Inc., 333 Lakeside Drive, Foster City, California 94404,[1] and XenoPort, Inc., 3410 Central Expressway, Santa Clara, California 95051[2]

Received 15 July 2004/Returned for modification 7 October 2004/Accepted 31 December 2004

An isopropylalaninyl monoamidate phenyl monoester prodrug of tenofovir (GS 7340) was prepared, and its in vitro antiviral activity, metabolism, and pharmacokinetics in dogs were determined. The 50% effective concentration (EC_{50}) of GS 7340 against human immunodeficiency virus type 1 in MT-2 cells was 0.005 μM compared to an EC_{50} of 5 μM for the parent drug, tenofovir. The (*L*)-alaninyl analog (GS 7340) was >1,000-fold more active than the (*D*)-alaninyl analog. GS 7340 has a half-life of 90 min in human plasma at 37°C and a half-life of 28.3 min in an MT-2 cell extract at 37°C. The antiviral activity (>10× the EC_{50}) and the metabolic stability in MT-2 cell extracts (>35×) and plasma (>2.5×) were also sensitive to the stereochemistry at the phosphorus. After a single oral dose of GS 7340 (10 mg-eq/kg tenofovir) to male beagle dogs, the plasma bioavailability of tenofovir compared to an intravenous dose of tenofovir was 17%. The total intracellular concentration of all tenofovir species in isolated peripheral blood mononuclear cells at 24 h was 63 μg-eq/ml compared to 0.2 μg-eq/ml in plasma. A radiolabeled distribution study with dogs resulted in an increased distribution of tenofovir to tissues of lymphatic origin compared to the commercially available prodrug tenofovir DF (Viread).

Highly active antiretroviral therapy (HAART) for the treatment of human immunodeficiency virus is effective in reducing plasma viral loads below current assay detection limits and is responsible for significant reductions in AIDS-related mortality in the United States (13). Combinations of protease and reverse transcriptase inhibitors are extremely potent at blocking de novo infection; however, they have no effect on latently infected cells. The half-lives of these latent cellular reservoirs were originally estimated to be >3 years, leading to the conclusion that it may not be possible to eradicate human immunodeficiency virus (HIV) from an infected individual by using current HAART (2). It has subsequently been shown that even in patients who have undetectable plasma viremia (<50 copies/ml), low-level replication is ongoing (11, 15, 36), resulting in repopulation of latent reservoirs and thus accounting for the long apparent half-lives observed (12, 22, 23, 35). The failure of HAART to completely shut down virus replication in vivo is a function of both the intrinsic potency of the drug regimen and its distribution to the cellular sites of virus replication. The lymphatic tissues and the peripheral blood mononuclear cells (PBMCs) are the primary sites of virus replication and potential virus latency (9, 19). A drug targeting strategy that selectively enhances active drug concentrations in these tissues without excessive systemic exposure is conceptually attractive and would potentially lead to a more effective HAART with fewer potential side effects.

* Coresponding author. Mailing address: Gilead Sciences, Inc., 333 Lakeside Dr., Foster City, CA 94404. Phone: (650) 522-5716. Fax: (650) 522-5899. E-mail: Bill_Lee@Gilead.com.

Tenofovir, {9-[(*R*)-2(phosphonomethoxy)propyl]adenine} (PMPA) (Fig. 1) is a nucleotide analog that inhibits HIV reverse transcriptase and shows potent in vitro and in vivo activity against HIV (3, 7) but has low oral bioavailability in preclinical models (6). An oral prodrug of tenofovir, tenofovir disoproxil fumarate (tenofovir DF; Viread) (Fig. 1), is indicated in combination with other antiretrovirals for the treatment of HIV infection. The long intracellular half-life (~50 h) of the active diphosphate metabolite of tenofovir in resting PBMCs (26) allows this drug to be administered once daily. The prodrug tenofovir DF was designed to undergo rapid metabolism to the parent drug, tenofovir, in the systemic circulation after oral administration. Interestingly, in preclinical studies with dogs, the intracellular levels of tenofovir in PBMCs were fivefold higher after oral administration of tenofovir DF than after an equivalent subcutaneous exposure of tenofovir. Correspondingly, in human clinical trials, the change in HIV virus load was threefold higher after oral administration of tenofovir DF than after an equivalent exposure of intravenously (i.v.) administered tenofovir (5). The "enhanced" anti-HIV activity observed in patients with the oral prodrug relative to the intravenously administered parent drug may be attributable to an increase in the intracellular concentration of tenofovir, which is likely the result of better intracellular distribution of the oral prodrug.

These results led us to explore a new class of orally administered tenofovir prodrugs designed to circulate systemically as the prodrug and to undergo selective conversion to tenofovir inside cells. In this report, we describe the in vitro and in vivo characterization of GS 7340, an isopropylalaninyl monoami-

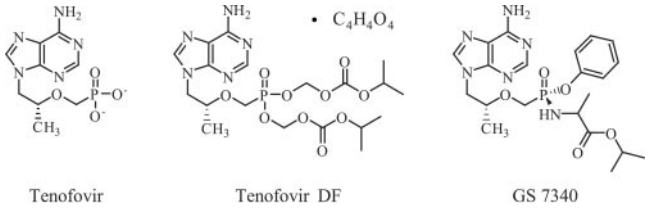

FIG. 1. Structure.

date phenyl monoester prodrug of tenofovir (Fig. 1). This molecule demonstrates extremely potent in vitro activity and selective targeting to lymphoreticular tissues and PBMCs in vitro and in vivo.

MATERIALS AND METHODS

Chemicals. The synthesis of tenofovir and tenofovir DF was described previously (1, 31). The monoamidate prodrugs of tenofovir were prepared by using a modified procedure from the literature (32). Detailed procedures and identification will be published elsewhere. The radiolabeled analogs [^{14}C]tenofovir DF (specific activity, 42 mCi/mmol) and [^{14}C]GS 7340 (specific activity, 53 mCi/mmol) were obtained from Moravek Biochemicals (Brea, Calif.). The radiochemicals were verified by high-performance liquid chromatography (HPLC) before use and were estimated to be >98% pure. All other chemicals and solvents were obtained from commercial sources.

In vitro antiviral activity and cytotoxicity. Triplicate serial dilutions of the test compounds were incubated in 96-well plates with MT-2 cells (20,000 cells/well) infected with HIV-1 IIIb at a multiplicity of infection of 0.01. After 5 days at 37°C, the virus-induced cytopathic effect was determined by using a colorimetric cell viability assay based on the metabolic conversion of 2,3,-bis(methoxy-4-nitro-5-sulfophenyl)-2H-tetrazolium-5-carboxanilide (XTT) as previously described in the literature (34). The concentration of each compound that inhibited the virus-induced cytopathic effect by 50% (EC_{50}) was estimated from the inhibition plots. To determine the compound cytotoxicity, uninfected MT-2 cells in 96-well plates (20,000 cells/well) were incubated with appropriate serial dilutions of tested compounds for 5 days, followed by the XTT-based cell viability assay. Cell growth was expressed as a percentage of the signal relative to untreated control. The concentration of each drug that reduced the cell growth by 50% was estimated from the inhibition plots.

In vitro metabolism studies. MT-2 cell extract was prepared from MT-2 cells according to a previously published procedure (21). Extract (80 μl) was transferred into a screw-cap centrifuge tube and incubated at 37°C for 5 min. Test compounds were dissolved in HEPES buffer (0.2 mg/ml) containing 0.010 M HEPES, 0.05 M potassium chloride, 0.005 M magnesium chloride, and 0.005 M DL-dithiothreitol, and 20 μl was added to the MT-2 cell extract. Aliquots (each, 20 μl) were taken at specified times and mixed with 60 μl of methanol containing 0.015 mg/ml of 2-hydroxymethylnaphthalene (internal standard). The mixture was centrifuged at 15,000 × *g* for 5 min, and the supernatant was analyzed by HPLC. The same procedure was employed for the human plasma (pooled from George King Biomedical Systems, Inc.), except that test compounds were dissolved in Tris-buffered saline containing 0.05 M Tris, 0.0027 M KCl, and 0.138 M NaCl (pH 7.5).

The reverse-phase gradient HPLC method used to analyze samples from the MT-2 cell extract and plasma metabolism studies employed a 4.6- by 250-mm, 5-μm particle size Zorbax R_x-C_8 column (MAC-MOD Analytical, Inc.; Chadds Ford, Pa.) with UV detection at 260 nM. The mobile phase was varied from 50 mM potassium phosphate (pH 6.0)/CH_3CN (95:5) to 50 mM potassium phosphate (pH 6.0)/CH_3CN (50:50) over 30 min at a flow rate of 1.0 ml/min.

Human whole blood was incubated for 1 h at 37°C separately with ^{14}C-radiolabeled GS 7340, tenofovir DF, and tenofovir at a concentration of 5 μg-eq tenofovir per ml (17.4 μM). The blood was subjected to treatment with the Ficoll-Paque sodium diatriozate solution (described below). The treatment resulted in the formation of multiple layers containing different cell types. The bottom layer contained mostly erythrocytes (RBCs) aggregated by Ficoll-Paque. The PBMC layer was washed and extracted with 70% methanol. Aliquots of the plasma and RBC layers (0.5 ml) were also extracted. Radioactivity in all layers was measured by oxidation/scintillation counting and by a comparison with radioactivity from the standard solutions. All extracts were reconstituted in water and analyzed by HPLC with radiometric flow detection (8). The experiment was repeated, incubating with [^{14}C]GS 7340 at 0.7, 2.3, 6.9, and 20.8 μM.

MT-2 cells (10^7) were incubated in a standard cell culture medium with 10 μM of [^{14}C]GS 7340 at 37°C for 24 h. At specified time points, an aliquot of the cell suspension was taken, and cells were counted, washed three times with ice-cold phosphate-buffered saline (PBS), and extracted with 70% methanol. The supernatants were analyzed using HPLC with radiometric flow detection (8).

Isolation of CD4$^+$ T cells and monocytes from whole blood. Whole human blood was incubated for 1 h at 37°C with 17.4 μM [^{14}C]GS 7340. PBMCs were obtained by density gradient centrifugation over Ficoll-Paque. CD4$^+$ T helper (Th) cells or monocytes were isolated from PBMCs by depletion of non-Th cells and nonmonocytes, respectively. The non-Th cells were indirectly magnetically labeled using a cocktail of hapten-conjugated CD8, CD11B, CD16, CD19, CD36, and CD56 antibodies and paramagnetic beads coupled to an anti-hapten monoclonal antibody (Miltenyi Biotec, Inc., Auburn, CA). For depletion of nonmonocytes, the T cells, NK cells, B cells, dendritic cells, and basophils from PBMCs were indirectly magnetically labeled using a cocktail of hapten-conjugated CD3, CD7, CD19, CD45RA, CD56 and anti-immunoglobulin antibodies and paramagnetic beads coupled to an anti-hapten monoclonal antibody. The magnetically labeled cells were depleted by retention on an extraction column in the magnetic field. The eluted respective cell types (CD4 or monocytes) were lysed and analyzed for tenofovir metabolites by radiochromatography (8).

In vivo administration and sample collection. The in-life phase was conducted in accordance with the recommendations of the *Guide for the Care and Use of Laboratory Animals* (National Institutes of Health publication 86-23) and was approved by the Institutional Animal Care and Use Committee at Stanford Research Institute (Menlo Park, CA). Male beagle dogs (four to six/group; body weight, 10 ± 2 kg) were used for the studies. Prodrugs were formulated as solutions in 50 mM citric acid and administered as a single dose by oral gavage. For PBMCs, blood samples were collected at 0 (predose), 2, 8, and 24 h postdose. For plasma, blood samples were collected at 0 (predose), 5, 15, and 30 min and 1, 2, 3, 4, 6, 8, 12, and 24 h postdose. Blood (1.0 ml) was processed immediately for plasma by centrifugation at 2,000 rpm for 10 min. Plasma samples were frozen and maintained at −70°C until analyzed.

PBMC preparation. Whole blood (8 ml) drawn at specified time points was mixed in equal proportion with PBS, layered onto 4 ml of Ficoll-Paque solution (Pharmacia Biotech), and centrifuged at 400 × *g* for 40 min. The PBMC layer was removed and washed once with PBS. The formed PMBC pellet was reconstituted in 0.5 ml of PBS, and cells were resuspended and counted with a hemocytometer. The number of cells multiplied by the mean single-cell volume was used to calculate intracellular concentrations. A reported value of 200 femtoliters was used as the resting PBMC volume (28).

Determination of tenofovir and GS 7340 and GS 7339 in plasma and PBMCs. The concentration of tenofovir in dog plasma samples was determined by derivatizing tenofovir with chloroacetaldehyde to yield a highly fluorescent N^1,N^6-ethenoadenine derivative (18). Plasma (100 μl) was mixed with 200 μl of 0.1% trifluoroacetic acid in acetonitrile to precipitate proteins. Samples were then evaporated to dryness under reduced pressure at room temperature. Dried samples were reconstituted in 200 μl of derivatization cocktail (0.34% chloroacetaldehyde in 100 mM sodium acetate, pH 4.5), vortexed, and centrifuged. The supernatant was then transferred to a clean screw-cap tube and incubated at 95°C for 40 min. Derivatized samples were then evaporated to dryness and reconstituted in 100 μl of water for HPLC analysis. Conversion of intact prodrug to tenofovir during the analysis procedures was determined to be <10% with prodrug standards.

Ribonucleotides present in the PBMC extracts were removed by selective oxidation using a modified procedure of Tanaka et al. (33). PBMC extracts were mixed 1:2 with methanol and evaporated to dryness under reduced pressure. The dried samples were derivatized with chloroacetaldehyde as described above for the plasma assay, mixed with 20 μl of 1 M rhamnose and 30 μl of 0.1 M sodium periodate, and incubated at 37°C for 5 min. Following incubation, 40 μl of 4 M methylamine and 20 μl of 0.5 M inosine were added, and samples were further incubated at 37°C for 30 min. Samples were then evaporated to dryness under reduced pressure and reconstituted in water for HPLC analysis. Independently, it was demonstrated that the chloroacetaldehyde derivatization and periodate oxidation resulted in <6% conversion of the mono- and diphosphate metabolites of tenofovir to the N^1,N^6-ethenoadenine derivative of tenofovir.

The HPLC system comprised a P4000 solvent delivery system with AS3000 autoinjector and F2000 fluorescence detector (Thermo Separation, San Jose, CA). The column was an Inertsil ODS-2 column (4.6 by 150 mm). The mobile phases were as follows: A, 5% acetonitrile in 25 mM potassium phosphate buffer with 5 mM tetrabutyl ammonium bromide, pH 6.0; B, 60% acetonitrile in 25 mM potassium phosphate buffer with 5 mM tetrabutyl ammonium bromide, pH 6.0.

TABLE 1. In vitro anti-HIV-1 activity (EC_{50}), cytotoxicity (CC_{50}), and in vitro metabolic stabilities of tenofovir and tenofovir prodrugs

Prodrug	EC_{50}[a] (μM)	CC_{50}[a] (μM)[b]	Selectivity index[b]	$t_{1/2}$ (min)[b]	
				MT-2 cell extract	Human plasma
Tenofovir	5.0 ± 2.6	6,000 ± 2,700	1,250	NR	NR
Tenofovir DF	0.05 ± 0.03	50 ± 28	1,000	70.7 ± 10.1	0.41 ± 0.20
GS 7171	0.01 ± 0.005	95 ± 37	9,500	ND	ND
GS 7339	0.06 ± 0.04	>100	>1,700	>1,000	231 ± 72
GS 7340	0.005 ± 0.002	40 ± 29	8,000	28.3 ± 7.4	90 ± 12
GS 7485 (D-Ala)	10 ± 4	ND	ND	>700	>200
GS 7160	10 ± 2.5	ND	ND	ND	ND

[a] The data represent means ± SD from two to four independent determinations.
[b] NR, not reactive; ND, not determined.

The flow rate was 2 ml/min, and the column temperature was maintained at 35°C by a column oven. The gradient profile was 90% A/10% B for 10 min for tenofovir, followed by 65% A/35% B for 10 min for GS 7340. Detection was by fluorescence with excitation at 236 nm and emission at 420 nm, and the injection volume was 10 μl. Data was acquired and stored by an Artemis data acquisition system (Beckman, Palo Alto, CA).

Pharmacokinetic calculations. C_{max} and T_{max} were observed values. Tenofovir exposures were expressed as areas under tenofovir concentration curves from zero to 24 h (AUC_{0-24}). The AUC values were calculated using the trapezoidal rule. All other pharmacokinetic parameters, including the elimination half-life, were calculated by noncompartmental methods using WinNonlin (Pharsight Corp., Mountain View, CA).

Tissue distribution study. Two male beagle dogs (each, 10 to 12 kg) were dosed orally (10 mg-eq tenofovir/kg; 30 to 35 μCi/kg) by gavage with [^{14}C]GS 7340 or [^{14}C]tenofovir DF. Dosing solutions of GS 7340 and tenofovir DF were prepared 1 h prior to dosing by dissolving necessary quantities of GS 7340 (fumarate salt) or tenofovir DF and dried [^{14}C]GS 7340 or [^{14}C]tenofovir disoproxil (radiolabeled free base) in 50 mM citric acid (pH 2.2). Urine, as well as cage rinse and feces, was collected at 24 h after administration. Plasma samples were obtained at 0, 0.0833, 0.25, 0.5, 1, 1.5, 2, 4, 6, 8, and 24 h postdose. Additionally, blood samples were collected at 0, 2, 8, and 24 h postdose and processed for PBMCs as described above. At 24 h after the dose, the animals were sacrificed, and tissues were removed for further analysis. Plasma, peripheral blood mononuclear cells, whole blood, bile, cerebrospinal fluid, and urine were analyzed for total radioactivity by oxidation. Feces were homogenized in water (10% [wt/wt]), and aliquots of homogenate were processed by oxidation for counting. The brain, liver, spleen, heart, lungs, kidneys, uterus, stomach, small intestines, stomach contents, small intestine contents, and large intestine contents were homogenized separately in water (20% [wt/wt]), and aliquots of each homogenate were oxidized and counted.

RESULTS

In vitro anti-HIV activity. GS 7340 was synthesized from (*R*)-PMPA and (*L*)-isopropyl alanine ester in a nonstereospecific synthesis, resulting in the formation of equal amounts of two stereoisomers at phosphorus. These two diastereomers, GS 7339 and GS 7340, were subsequently separated by chromatography. To assess the ability of these prodrugs to cross the cellular membrane and undergo intracellular metabolism to tenofovir, their in vitro activities were measured against HIV-1 in MT-2 cells. The antiviral activities for the diastereomeric mixture (GS 7171), the individual diastereomers (GS 7339 and GS 7340), the diastereomic mixture of D-alaninyl analog (GS 7485), and the alaninyl monoamidate metabolite (GS 7160) are shown in Table 1. Compared to tenofovir, the individual isomers, GS 7339 and GS 7340, were 83- and 1,000-fold more active, respectively, whereas the D-isopropyl alaninyl analog (GS 7485) and the metabolite (GS 7160) showed activity similar to tenofovir. The enhanced activities of the L-alaninyl prodrugs compared to those of tenofovir are a result of greater cellular permeability and rapid conversion to tenofovir inside the MT-2 cells. The dramatically reduced activity (1,000 fold) of the D-alaninyl analog (GS 7485), relative to the L-alaninyl analog (GS 7171) demonstrates a strong metabolic preference inside the MT-2 cells for the L-amino acid (see below). The 12-fold-greater activity of GS 7340 compared to that of GS 7339 further suggests that intracellular metabolism is also sensitive to stereochemistry at the phosphorus. The greater selectivity index (~10×) for GS 7340 than tenofovir DF may reflect the kinetics of cell loading; GS 7340 results in a higher initial intracellular concentration of tenofovir, which may differentially affect antiviral potency and cytotoxicity.

In vitro metabolism and accumulation in PBMCs. The antiviral activities in tissue culture were determined in buffer containing 5% heat-inactivated fetal calf serum, a medium in which the prodrugs in this study were stable. To enhance the in vivo accumulation of tenofovir inside cells, a prodrug must exhibit greater stability in plasma relative to the intracellular environment. Table 1 lists the in vitro half-lives of the monoamidate prodrugs and tenofovir DF in MT-2 cell extract and human plasma. GS 7340 was metabolized 3-fold faster in MT-2 cell extract than in plasma, whereas tenofovir DF, a prodrug designed to release tenofovir into systemic circulation, was metabolized 170-fold faster in plasma. As inferred from the antiviral activity, GS 7339 and the D-amino acid analogs (GS 7485) are more stable in MT-2 cell extract than plasma.

The putative first step in the conversion of the GS 7340 to tenofovir is the hydrolysis of the amino acid ester, which is sensitive to stereochemistry at both the amino acid and phosphorus. The metabolites observed from the degradation of GS 7340 were identified as the alaninyl amidate (GS 7160) in MT-2 cell extract and the isopropyl alaninyl amidate (GS 7161) in plasma (Fig. 2) by coinjection of authentic samples prepared independently. In the MT-2 cell extract, the alaninyl amidate metabolite was slowly hydrolyzed to tenofovir. No evidence of further conversion to the mono- or diphosphate metabolites was observed in the MT-2 cell extracts.

The metabolism of GS 7340 was further explored by incubating [^{14}C]GS 7340 in fresh whole human blood. After a 1-h incubation at 37°C, plasma, PBMCs, and RBCs were separated and total radioactivity was analyzed by HPLC with radiometric detection. The results are shown in Table 2, along with those of tenofovir and tenofovir DF. The total recovered radioactivity in PBMCs after a 1-h incubation with GS 7340 was 9.3-fold and 38-fold higher than with tenofovir DF or tenofovir, respec-

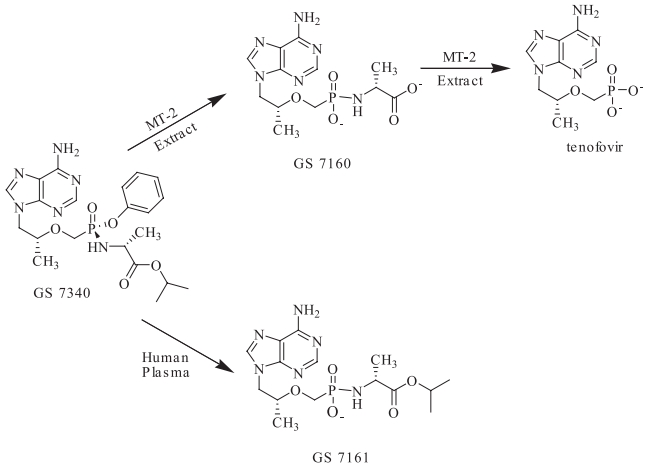

FIG. 2. Routes of metabolism.

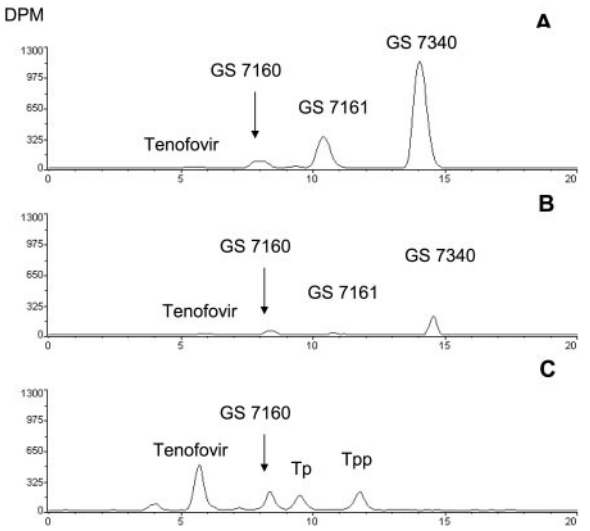

FIG. 3. Radiochromatograms labeled with ^{14}C from plasma (A), aggregated red blood cells (B), and PBMCs (C), obtained after incubation of 17.4 μM GS 7340 with whole human blood for 1 h at 37°C.

tively. The greater radioactivity in RBCs after incubation with GS 7340 or tenofovir DF than with tenofovir can be accounted for by the decreased permeability of the latter across RBC membrane. The HPLC radiochromatograms depicting the product distribution in PBMCs, plasma, and RBCs after incubation of GS 7340 in whole blood are shown in Fig. 3. In plasma, the major species present was intact GS 7340 (84%), with minor amounts of GS 7161 (13%), GS 7160 (2%), and tenofovir (1%). In RBCs, the major species observed was intact GS 7340 (57%). In PBMCs, there was no intact GS 7340 detected, and the major species present were tenofovir (45%), tenofovir monophosphate (16%), tenofovir diphosphate (21%), and GS 7160 (18%). The phosphorylation of tenofovir in PMBCs to the mono- and diphosphate species after 1-h incubation in whole blood was not saturable over a 30-fold concentration range (Fig. 4). Additionally, in MT-2 cells incubated with 10 μM GS 7340, the formation of the diphosphate metabolite was linear out to 24 h (Fig. 5.) The concentration of the diphosphate species inside the MT-2 cells at 24 h exceeded the initial extracellular concentration of GS 7340 by 250 fold. These results are consistent with the data generated in MT-2 extract and isolated plasma; however, unlike the MT-2 extract, conversion to the active diphosphate metabolite was readily observed with intact MT-2 cells and PBMCs.

The whole-blood experiments were extended to determine the distribution of tenofovir into $CD4^+$ T lymphocyte and monocyte fractions isolated from the PBMCs, following incubation with radiolabeled GS 7340. The results in Table 3 show that the concentration of total GS 7340 metabolites in $CD4^+$ cells was approximately 70% of that in the entire PBMC fraction. The concentration of total GS 7340 metabolites in monocytes was approximately half of that in $CD4^+$ cells. There are no major differences in the relative concentration of phosphorylated tenofovir species in $CD4^+$ cells or monocytes.

In vivo pharmacokinetics in samples from dogs. The diastereomeric mixture, GS 7171, was administered as an oral solution in 50 mM citric acid (pH 2.3) at a dose of 10 mg-eq/kg (of tenofovir) to five male beagle dogs. Figure 6 shows the resulting plasma levels of tenofovir and the individual diastereomers (GS 7339 and GS 7340) from 0 to 24 h after administration. Elimination of both diastereomers (GS 7340 and GS 7339) was rapid relative to tenofovir in plasma. Consistent with the faster metabolism observed in vitro (Table 1), GS 7340 was cleared more quickly from plasma than GS 7339. To measure the intracellular levels of tenofovir after oral administration of GS 7171, PBMCs were isolated from dog blood samples at 0, 2, 8, and 24 h postadministration. After cells were counted, the concentration of tenofovir in the PBMCs was analyzed by a

TABLE 2. Distribution of all tenofovir-related species after incubation of ^{14}C-labeled drug in human whole blood[a]

Drug	Total amt recovered[b] (μg-eq)		
	Plasma	PBMC	RBC
GS 7340	43.0 ± 7.8	1.25 ± 0.22	12.6 ± 3.02
Tenofovir DF	48.10 ± 8.7	0.133 ± 0.029	10.5 ± 5.17
Tenofovir	55.70 ± 4.5	0.033 ± 0.014	3.72 ± 1.86

[a] A total of 10 μg-eq/ml of ^{14}C-labeled compound was incubated for 1 h at 37°C in human blood, followed by Ficoll-Paque separation of the blood fractions.
[b] Mean ± SD, $n = 3$.

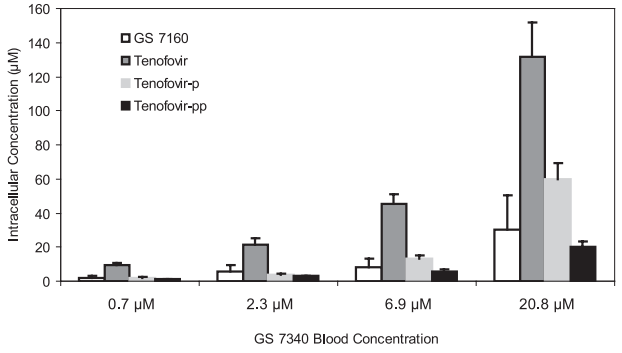

FIG. 4. Metabolism of [^{14}C]GS 7340 in PMBCs after 1-h incubation in whole human blood at 37°C (mean ± SD; $n = 3$ samples of whole blood).

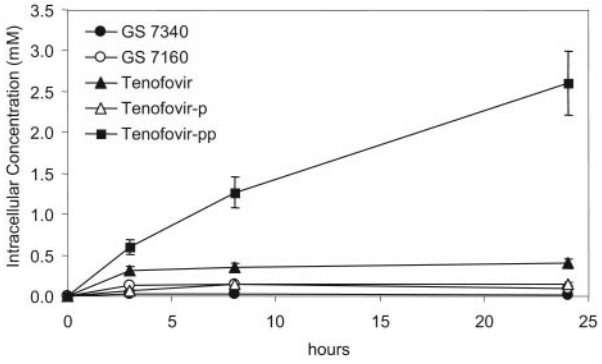

FIG. 5. Formation of tenofovir and metabolites in MT-2 cells during a 24-h incubation with 10 μM [^{14}C]GS 7340 (mean ± SD; $n = 3$ samples of MT-2 cells).

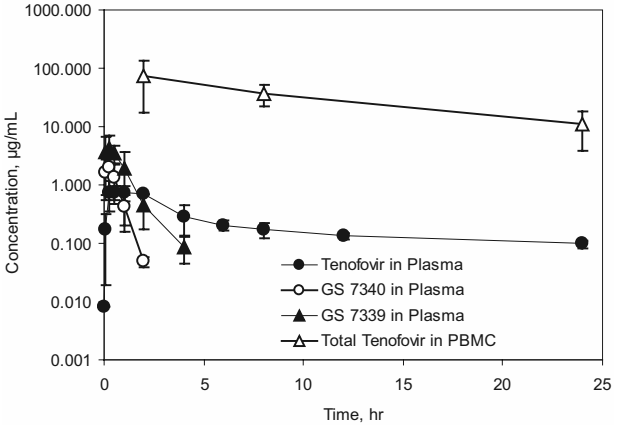

FIG. 6. Mean concentration versus time profiles for tenofovir, GS 7340, and GS 7339 in plasma and tenofovir in PBMCs after oral administration of GS 7171 (10 mg-eq/kg tenofovir) to dogs (mean ± SD for samples from four dogs).

precolumn fluorescent derivatization reverse-phase HPLC method (18). Tenofovir concentration in PBMCs increased rapidly within 2 h to levels that greatly exceeded plasma levels (Fig. 6). The ratio of the total tenofovir AUC from 0 to 24 h in PBMCs to that in plasma was >90 after a single dose of GS 7171. GS 7339 and GS 7340 were also administered separately to two sets of five dogs (10 mg-eq/kg of tenofovir). A bar graph comparing the plasma and PBMC $AUC_{0\text{-}24}$ values for tenofovir after administration of GS 7340, GS 7339, GS 7171, and tenofovir DF is shown in Fig. 7. Oral administration of GS 7340, the more rapidly cleared isomer, resulted in a >34-fold increase in the $AUC_{0\text{-}24}$ in PBMCs relative to tenofovir DF and a 6-fold increase relative to GS 7339. In the case of tenofovir DF, the $AUC_{0\text{-}24}$ ratio of tenofovir in PBMCs to plasma was 4.7. Based on these data and in vitro metabolism studies, the more rapidly cleared isomer GS 7340 was chosen as a lead prodrug for further preclinical development.

The concentration of tenofovir in PBMCs determined by the fluorescent derivatization method does not include the tenofovir mono- or diphosphate species. As part of the radiolabeled distribution study (see below), PBMCs were collected at 2, 8, and 24 h, and total radioactivity was determined. The concentration of total tenofovir metabolites at 24 h was 63 μg-eq/ml. The calculated $t_{1/2}$ value in PBMCs was ~25 h, which is consistent with the intracellular half-life observed in vitro with resting lymphocytes (26).

The absolute bioavailabilities of tenofovir after oral administration of GS 7171, GS 7339, and GS 7340 were calculated by comparing the resulting plasma tenofovir $AUC_{0\text{-}24}$ to that observed after the i.v. administration of tenofovir itself. Data are shown in Table 4. The bioavailabilities were 20, 13, and 17%, respectively. The oral bioavailability of the prodrug (as prodrug) was >70% at the 20-mg/kg dose and was calculated by comparing the plasma levels of GS 7340 after oral administration to those after an i.v. bolus administration of GS 7340 (data not shown).

Tissue distribution of GS 7340 after oral administration in dogs. The results of a tissue distribution study in dogs following oral administration of [^{14}C]GS 7340 or [^{14}C]tenofovir DF are shown in Table 5. Two dogs per group received a single oral dose (10 mg-eq/kg; 35 μCi/kg), and tissues were harvested at 24 h postadministration. Except for the kidney and liver, radioactivity was generally higher in all tissues after administration of GS 7340 than with tenofovir DF. In the lymph nodes, concentrations of radioactivity were 5- to 15-fold higher after administration of GS 7340. In lung, ileum, spleen, bone marrow, and muscle, concentrations were consistently higher than with tenofovir DF. The increased concentrations of radioactivity in the bile for GS 7340 suggest that there is a hepatic

TABLE 3. Concentration of metabolites in CD4$^+$ lymphocytes and monocytes isolated from whole human blood after incubation with 17 μM ^{14}C-labeled GS 7340 for 1 h

Cell type	Intracellular concn[a] (μM)				Total concn (μM)
	Tenofovir	Tenofovir-P	Tenofovir-PP	GS 7340	
CD4^{+}[b]	218 ± 31	122 ± 8	157 ± 15	0	703 ± 36
Monocytes[b]	138 ± 55	89 ± 8	73 ± 15	0	364 ± 24
PBMCs[c]	ND[d]	ND	ND	ND	921 ± 64

[a] Values are means ± SD ($n = 2$ samples of whole blood).
[b] Calculated based on cell volumes of 0.2 pl/cell for T lymphocytes and 0.4 pl/cell for monocytes (4).
[c] Based on average volume of 0.2 pl/cell.
[d] ND, not determined.

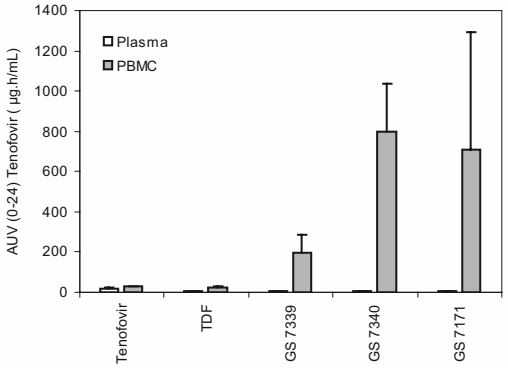

FIG. 7. Tenofovir in PBMCs and plasma ($AUC_{0\text{-}24\ h}$) after subcutaneous administration of tenofovir and after oral administration of tenofovir DF, GS 7339, GS 7340, and GS 7171 (10 mg-eq/kg) to dogs (mean ± SD, $n = 5$ dogs).

TABLE 4. Pharmacokinetics of tenofovir in plasma after oral administration of GS 7340, GS 7339, and GS 7171 in fasted dogs[a]

Drug (route)	AUC_{0-24} (μg · h/ml)	C_{max} (μg/ml)	T_{max} (h)	$t_{1/2}$ (h)	%F[d]
GS 7340 (p.o.)[b]	7.88 (2.24)	0.82 (0.17)	1.0 (0.0)	23.2 (12.9)	16.9 (4.8)
GS 7339 (p.o.)[b]	6.14 (2.06)	0.94 (0.21)	1.25 (0.5)	10.4 (2.2)	13.1 (4.4)
GS 7171 (p.o.)[c]	8.17 (1.2)	0.91 (0.21)	0.94 (0.79)	20 (4)	19.7 (2.8)

[a] Data are means ± SD for groups of five dogs. p.o., oral.
[b] Dose as tenofovir (mg-eq/kg) = 10.85.
[c] Dose as tenofovir (mg-eq/kg) = 9.64.
[d] %F calculated from $AUC_{0-\infty}$ = 4.30 μg-h/ml for a 1-mg/kg dose of intravenous tenofovir.

clearance mechanism for either the intact prodrug or the metabolites.

DISCUSSION

Although there is still much debate regarding the ultimate reservoir for HIV, the evidence for ongoing HIV replication during HAART in patients who have undetectable viremia is compelling. Using an ultrasensitive viral RNA assay, Ramratnam et al. have shown that low-level viral bursts can be detected in samples from stable, long-term patients on HAART (22). The number of bursts observed over a 6-month period was directly correlated to the terminal viral elimination half-life from plasma. These data suggest that the long apparent half-lives (>44 mo) reported for "latent cells" (10) may be an overestimation of the true latency half-life, since new latent cells are being formed as a result of low-level virus replication. More-potent HAART therapies or therapies that better target the sites of ongoing HIV replication are required to completely halt virus replication. Currently, the intrinsic potencies of potential drugs are optimized against HIV in tissue culture systems with PBMCs or immortalized cell lines to replicate the virus. These assays are very useful for optimizing chemical structure during the initial phases of drug design; however, they do not provide any guidance into the pharmacokinetics, intracellular half-life, or distribution of a drug in vivo. Intracellular half-life and distribution are particularly important because a significant fraction of memory $CD4^+$ T cells exists outside of lymphoid tissue (24). Additionally, suboptimal drug concentrations in replication competent compartments will select and amplify resistant virus (14, 25).

Tenofovir belongs to a class of nucleotide analogs that have prolonged intracellular half-lives (20). The long intracellular half-life of tenofovir is a result of rapid metabolism within the cell to the nucleotide diphosphate and its limited efflux from cells. The phosphonate moiety of tenofovir is recognized by cellular kinases as a monophosphate, thereby bypassing the initial phosphorylation step, which can be rate limiting for nucleoside analogs (25). Because tenofovir is a dianion at physiological pH, it has low cellular permeability, which is reflected in its in vitro HIV-activity (EC_{50} = 5 μM). However, in vivo, the long intracellular half-life of tenofovir results in a potent and durable anti-HIV effect in both preclinical models and clinical studies (30). The amidate prodrug GS 7340 was designed to overcome the permeability limitations of tenofovir by masking the dianion with a neutral promoiety and increasing the plasma stability of the prodrug relative to its intracellular stability. The in vitro anti-HIV potency of GS 7340 (EC_{50} = 0.005 μM) is comparable to the most potent protease inhibitors and reflects the greater cell permeation of GS 7340 compared to tenofovir. In addition to favorable potency and a long intracellular half-life, the in vivo administration of GS 7340 results in an enhanced distribution to lymphatic tissue compared to tenofovir DF. The concentration of tenofovir inside PBMCs at 24 h was >100 fold the concentration of tenofovir in plasma at the same time point, and the ratio of AUC_{0-24} for tenofovir in PBMCs versus plasma was >150 (Fig. 7). With tenofovir DF, the PBMC/plasma ratio for $AUC_{0-24\ h}$ was 5. Since the HPLC assay only measured tenofovir inside PBMCs and not the mono- or diphosphate species, these differences should be considered the minimum ratios. Using total reactivity at 24 h to compare the PBMC-to-plasma concentration, the ratio for GS 7340 was 316, suggesting that the majority of the tenofovir species inside cells exists as mono- or diphosphate.

In our drug optimization studies, we used PBMCs as a surrogate marker for distribution to lymphatic tissues, since the exchange of lymphocytes between blood and lymph is rapid and only a small percentage of the total lymphocytes reside in the blood compartment. The increased concentration of radioactivity in the lymph nodes, ileum, lung, bone marrow, and thymus after administration of GS 7340 relative to tenofovir DF suggests that the amidate is preferentially metabolized to tenofovir and accumulates in tissues that contain high concentrations of lymphatic cells. Although we do not have detailed cellular distribution data for these tissues, the fact that tenofovir is present in tissues that have all been implicated as possible HIV reservoirs is encouraging. It must be noted, however, that the expanded distribution and the higher intracellular levels of tenofovir after administration of GS 7340 open the possibility of safety issues not observed with tenofovir DF.

Other in vitro studies have been published using an amidate prodrug approach to mask the monophosphates of zidovudine (AZT) and stavudine (d4T). The monoamidate prodrugs of the monophosphate of AZT exhibit minimal or no enhancement in in vitro anti-HIV activity (16, 17). The modest in vitro effects seen with these AZT prodrugs have been explained in part by the lability of the AZT monophosphate bond, which can readily hydrolyze back to AZT. Selected amidate prodrugs of d4T monophosphate do show significant increases in in vitro activity relative to that of d4T itself (up to 100 fold), suggesting that the subsequent phosphorylation is rapid compared to the hydrolysis of the nucleoside phosphate bond (29). The principal advantage of this approach with nucleosides is the ability to deliver the nucleoside monophosphate into the cell, thereby removing a potential rate-limiting step in the formation of the nucleoside triphosphate. The half-life of the nucleoside in cells is unchanged.

TABLE 5. Tissue distribution of ^{14}C-labeled tenofovir DF and ^{14}C-labeled GS 7340 in dogs following an oral dose of tenofovir of 10 mg-eq/kg[a]

Tissue or fluid	Tenofovir DF		GS 7340		Tissue concn ratio of GS 7340 to tenofovir DF
	% Dose	Concn (μg-eq/g)[b]	% Dose	Concn (μg-eq/g)[b]	
Liver	12.40	38.3 ± 14.3	16.45	52.9 ± 4.7	1.4
Kidney	4.58	87.9 ± 38.4	3.78	80.2 ± 3.4	0.9
Lungs	0.03	0.53 ± 0.06	0.34	4.34 ± 0.15	8.2
Iliac lymph nodes	<0.01	0.51 ± 0.14	0.01	5.42 ± 0.86	10.6
Axillary lymph nodes	<0.01	0.37 ± 0.25	0.01	5.54 ± 0.42	14.8
Inguinal lymph nodes	<0.01	0.28 ± 0.28	<0.01	4.12 ± 0.44	15.0
Mesenteric lymph nodes	<0.01	1.20 ± 0.64	0.04	6.88 ± 0.78	5.7
Thyroid gland	<0.01	0.30 ± 0.20	<0.01	4.78 ± 1.31	15.8
Pituitary gland	<0.01	0.23 ± 0.07	<0.01	1.80 ± 0.13	7.8
Salivary gland (left + right)	<0.01	0.45 ± 0.1	0.03	5.54 ± 0.10	12.3
Adrenal gland	<0.01	1.9 ± 0.79	<0.01	3.47 ± 0.13	1.8
Spleen	<0.01	0.63 ± 0.11	0.17	8.13 ± 0.19	12.8
Pancreas	<0.01	0.57 ± 0.62	0.01	3.51 ± 0.57	6.2
Prostate	<0.01	0.24 ± 0.03	<0.01	2.14 ± 0.38	9.1
Testes (left + right)	0.02	1.95 ± 0.84	0.02	1.99 ± 0.74	1.0
Skeletal muscle	<0.01	0.11 ± 0.00	0.01	1.12 ± 0.17	10.1
Heart	0.03	0.46 ± 0.17	0.15	1.97 ± 0.03	4.3
Femoral bone	<0.01	0.08 ± 0.03	<0.01	0.28 ± 0.05	3.5
Bone marrow	<0.01	0.2 ± 0.08	<0.01	2.05 ± 0.92	10.2
Skin	<0.01	0.13 ± 0.06	<0.01	0.95 ± 0.17	7.2
Abdominal fat	<0.01	0.16 ± 0.01	<0.01	0.90 ± 0.07	5.8
Eye (left + right)	<0.01	0.06 ± 0.03	<0.01	0.24 ± 0.00	3.7
Brain	<0.01	<LOD	<0.01	<LOD	ND
Cerebrospinal fluid	<0.01	<LOD	<0.01	<LOD	ND
Spinal cord	<0.01	<LOD	<0.01	0.04 ± 0.00	ND
Stomach	0.11	1.93 ± 1.03	0.26	2.68 ± 0.27	1.4
Jejunum	1.34	3.01 ± 1.37	0.79	4.16 ± 0.73	1.4
Duodenum	0.49	4.96 ± 0.54	0.44	8.77 ± 1.13	1.8
Ileum	0.01	0.50 ± 0.19	0.16	4.61 ± 1.91	9.2
Large intestine	1.63	2.57 ± 0.33	2.65	47.2 ± 42.2	7.9
Gall bladder	<0.01	3.58 ± 1.99	0.04	25.0 ± 4.7	7.0
Bile	<0.01	9.63 ± 9.42	0.22	40.5 ± 4.9	4.2
Feces	40.96	ND	0.19	ND	NA
Total GI tract contents	5.61	ND	21.64	ND	NA
Urine	23.72	ND	14.73	91.9 ± 34.0	NA
Plasma at 24 h	<0.01	0.20 ± 0.09	<0.01	0.20 ± 0.02	1.0
PBMCs at 24 h[c]	<0.01	ND	<0.01	63.2 ± 15.5	ND
Whole blood at 24 h	<0.01	0.85 ± 0.20	0.16	0.20 ± 0.00	0.2
Total recovery	81.10		68.96		

[a] NA, not applicable; ND, not determined; <LOD, below the limit of detection (0.02 μg-eq/g).
[b] Concentrations are means ± SD for groups of two dogs.
[c] Calculated using typical recovery of 15×10^6 cells total and mean PBMC volume of 0.2 picoliters/cell.

The detailed mechanism for the selective intracellular targeting of the amidate prodrugs is not fully understood. However, we have shown that the monoamidate prodrugs of tenofovir are more rapidly cleaved in the intracellular environment than in plasma and that the tenofovir formed within the cell is rapidly phosphorylated to give a long-lived metabolite. The selectivity exhibited between plasma and intracellular extracts is the basis for the preferential cellular loading observed in vivo. The limited structure activity relationship presented in this study demonstrates that the intracellular degradation of the amidate prodrugs is sensitive to the stereochemistry at both the amino acid and the phosphorus, suggesting that the process is enzyme mediated. It has yet not been possible under buffer or enzymatic conditions to isolate the monophenyl monoamidate species, leading to the conclusion that this reaction is spontaneous. Work by other investigators with the monoami-

dates of nucleosides has identified a cytosolic fraction from hepatocytes thought to be responsible for cleavage of the P-N bond (27). However, in the case of GS 7160, degradation at low pH is extremely fast ($t_{1/2} < 1$ min); therefore, the spontaneous hydrolysis of the metabolite in a cellular compartment with a low pH cannot be ruled out. Investigations to characterize the specific enzymes and mechanism responsible for the conversion of the prodrug to tenofovir are in progress. The preferential distribution into PBMCs and other lymphatic tissues is likely due to the increased metabolic activity of these tissues and the long intracellular half-lives of tenofovir and its mono- and diphosphate metabolites.

In conclusion, the high concentrations of tenofovir observed in lymphatic tissues after oral administration of GS 7340 are expected to result in increased clinical potency relative to tenofovir DF and could have a profound effect on the low-level virus replication that occurs in tissues with suboptimal drug exposure during HAART. The parent drug, tenofovir, is unique in this potential, due to its long half-life as the active diphosphate in uninfected cells and the lack of significant in vivo resistance development. With GS 7340, it should be possible to reduce the total dose of tenofovir, thereby minimizing systemic exposure, while at the same time increasing antiviral activity.

REFERENCES

1. **Arimilli, M., C. Kim, and N. Bischofberger.** 1997. Synthesis, in vitro biological evaluation and oral bioavailability of 9-[2-(phosphonomethoxy)-propyl]adenine (PMPA) prodrugs. Antivir. Chem. Chemother. **8:**557–564.
2. **Arnaout, R. A., A. L. Lloyd, T. R. O'Brien, J. J. Goedert, J. M. Leonard, and M. A. Nowak.** 1999. A simple relationship between viral load and survival time in HIV-1 infection. Proc. Natl. Acad. Sci. USA **96:**11549–11553.
3. **Balzarini, J., A. Holy, J. Jindrich, L. Naesens, R. Snoeck, D. Schols, and E. De Clercq.** 1993. Differential antiherpesvirus and antiretrovirus effects of the (*S*) and (*R*) enantiomers of acyclic nucleoside phosphonates: potent and selective in vitro and in vivo antiretrovirus activities of (*R*)-9-(2-phosphonomethoxypropyl)-2, 6-diaminopurine. Antimicrob. Agents Chemother. **37:**332–338.
4. **Chapman, E. H., A. S. Kurec, and F. R. Davey.** 1981. Cell volumes of normal and malignant mononuclear cells. J. Clin. Pathol. **34:**1083–1090.
5. **Cundy, K. C.** 1999. Presented at the 7th European Conference on Clinical Aspects and Treatment of HIV Infection, Lisbon, Portugal, 23 to 27 October 1999.
6. **Cundy, K. C., C. M. Sueoka, G. R. Lynch, L. Griffin, W. A. Lee, and J.-P. Shaw.** 1998. Pharmacokinetics and bioavailability of the anti-human immunodeficiency virus nucleotide analog 9-[(*R*)-2-(phosphonomethoxy)propyl] adenine (PMPA) in dogs. Antimicrob. Agents Chemother. **42:**687–690.
7. **Deeks, S. G., P. Barditch-Crovo, P. S. Lietman, F. Hwang, K. C. Cundy, J. F. Rooney, N. S. Hellmann, S. Safrin, and J. O. Kahn.** 1998. Safety, pharmacokinetics, and antiretroviral activity of intravenous 9-[2-(*R*)-(phosphonomethoxy)propyl]adenine, a novel anti-human immunodeficiency virus (HIV) therapy, in HIV-infected adults. Antimicrob. Agents Chemother. **42:**2380–2384.
8. **Eisenberg, E. J., G.-X. He, and W. A. Lee.** 2001. Metabolism of GS-7340, a novel phenyl monophosphoramidate intracellular prodrug of PMPA, in blood. Nucleosides Nucleotides Nucleic Acids **20:**1091–1098.
9. **Embretson, J., M. Zupancic, J. L. Ribas, A. Burke, P. Racz, K. Tenner-Racz, and A. T. Haase.** 1993. Massive covert infection of helper T lymphocytes and macrophages by HIV during the incubation period of AIDS. Nature **362:** 359–362.
10. **Finzi, D., J. Blankson, J. D. Siliciano, J. B. Margolick, K. Chadwick, T. Pierson, K. Smith, J. Lisziewicz, F. Lori, C. Flexner, T. C. Quinn, R. E. Chaisson, E. Rosenberg, B. Walker, S. Gange, J. Gallant, and R. F. Siliciano.** 1999. Latent infection of CD4+ T cells provides a mechanism for lifelong persistence of HIV-1, even in patients on effective combination therapy. Nat. Med. **5:**512–517.
11. **Furtado, M. R., D. S. Callaway, J. P. Phair, K. J. Kunstman, J. L. Stanton, C. A. Macken, A. S. Perelson, and S. M. Wolinsky.** 1999. Persistence of HIV-1 transcription in peripheral-blood mononuclear cells in patients receiving potent antiretroviral therapy. N. Engl. J. Med. **340:**1614–1622.
12. **Grossman, Z., M. Polis, M. B. Feinberg, Z. Grossman, I. Levi, S. Jankelevich, R. Yarchoan, J. Boon, F. de Wolf, J. M. A. Lange, J. Goudsmit, D. S. Dimitrov, and W. E. Paul.** 1999. Ongoing HIV dissemination during HAART. Nat. Med. **5:**1099–1104.
13. **Hammer, S. M., K. E. Squires, M. D. Hughes, J. M. Grimes, L. M. Demeter, J. S. Currier, J. J. Eron, Jr., J. E. Feinberg, H. H. Balfour, Jr., L. R. Deyton, J. A. Chodakewitz, M. A. Fischl, and the AIDS Clinical Trials Group 320 Study Team.** 1997. A controlled trial of two nucleoside analogues plus indinavir in persons with human immunodeficiency virus infection and CD4 cell counts of 200 per cubic millimeter or less. N. Engl. J. Med. **337:**725–733.
14. **Kepler, T. B., and A. S. Perelson.** 1998. Drug concentration heterogeneity facilitates the evolution of drug resistance. Proc. Natl. Acad. Sci. USA **95:**11514–11519.
15. **Lewin, S. R., M. Vesanen, L. Kostrikis, A. Hurley, M. Duran, L. Zhang, and M. Markowitz.** 1999. Use of real-time PCR and molecular beacons to detect virus replication in human immunodeficiency virus type 1-infected individuals on prolonged effective antiretroviral therapy. J. Virol. **73:**6099–6103.
16. **McGuigan, C., R. N. Pathirana, S. S.-M. Choi, D. Kinchington, and T. J. O'Connor.** 1993. Phosphoramidate derivatives of AZT as inhibitors of HIV: studies on the carboxyl terminus. Antivir. Chem. Chemother. **4:**97–101.
17. **McIntee, E. J., R. P. Remmel, R. F. Schinazi, T. W. Abraham, and C. R. Wagner.** 1997. Probing the mechanism of action and decomposition of amino acid phosphomonoester amidates of antiviral nucleoside prodrugs. J. Med. Chem. **40:**3323–3331.
18. **Naesens, L., J. Balzarini, and E. De Clercq.** 1992. Acyclic adenine nucleoside phosphonates in plasma determined by high-performance liquid chromatography with fluorescence detection. Clin. Chem. **38:**480–485.
19. **Pantaleo, G., C. Graziosi, J. F. Demarest, L. Butini, M. Montroni, C. H. Fox, J. M. Orenstein, D. P. Kotler, and A. S. Fauci.** 1993. HIV infection is active and progressive in lymphoid tissue during the clinically latent stage of disease. Nature **362:**355–358.
20. **Pauwels, R., J. Balzarini, D. Schols, M. Baba, J. Desmyter, I. Rosenberg, A. Holy, and E. De Clercq.** 1988. Phosphonylmethoxyethyl purine derivatives, a new class of anti-human immunodeficiency virus agents. Antimicrob. Agents Chemother. **32:**1025–1030.
21. **Pompon, A., I. Lefebvre, J.-L. Imbach, S. Kahn, and D. Farquhar.** 1994. Decomposition pathways of the mono- and bis(pivaloyloxymethyl) esters of azidothymidine 5′-monophosphate in cell extract and in tissue culture medium: an application of the 'on-line ISRP-cleaning' HPLC technique. Antivir. Chem. Chemother. **5:**91–98.
22. **Ramratnam, B., J. E. Mittler, L. Zhang, D. Boden, A. Hurley, F. Fang, C. A. Macken, A. S. Perelson, M. Markowitz, and D. D. Ho.** 2000. The decay of the latent reservoir of replication-competent HIV-1 is inversely correlated with the extent of residual viral replication during prolonged anti-retroviral therapy. Nat. Med. **6:**82–85.
23. **Ramratnam, B., R. Ribeiro, T. He, C. Chung, V. Simon, J. Vanderhoeven, A. Hurley, L. Zhang, A. S. Perelson, D. D. Ho, and M. Markowitz.** 2004. Intensification of antiretroviral therapy accelerates the decay of the HIV-1 latent reservoir and decreases, but does not eliminate, ongoing virus replication. J. Acquir. Immune Defic. Syndr. Hum. Retrovirol. **35:**33–37.
24. **Reinhardt, R. L., A. Khoruts, R. Merica, T. Zell, and M. K. Jenkins.** 2001. Visualizing the generation of memory CD4 T cells in the whole body. Nature **410:**101–105.
25. **Richman, D. D.** 1996. The implications of drug resistance for strategies of combination antiviral chemotherapy. Antiviral Res. **29:**31–33.
26. **Robbins, B. L., R. V. Srinivas, C. Kim, N. Bischofberger, and A. Fridland.** 1998. Anti-human immunodeficiency virus activity and cellular metabolism of a potential prodrug of the acyclic nucleoside phosphonate 9-*R*-(2-phosphonomethoxypropyl)adenine (PMPA), bis(isopropyloxymethylcarbonyl) PMPA. Antimicrob. Agents Chemother. **42:**612–617.
27. **Saboulard, D., L. Naesens, D. Cahard, A. Salgado, R. Pathirana, S. Velazquez, C. McGuigan, E. De Clercq, and J. Balzarini.** 1999. Characterization of the activation pathway of phosphoramidate triester prodrugs of stavudine and zidovudine. Mol. Pharmacol. **56:**693–704.
28. **Segel, G. B., G. R. Cokelet, and M. A. Lichtman.** 1981. The measurement of lymphocyte volume: importance of reference particle deformability and counting solution tonicity. Blood **57:**894–899.
29. **Siddiqui, A. Q., C. Ballatore, C. McGuigan, E. De Clercq, and J. Balzarini.** 1999. The presence of substituents on the aryl moiety of the aryl phosphoramidate derivative of d4T enhances anti-HIV efficacy in cell culture: A structure-activity relationship. J. Med. Chem. **42:**393–399.
30. **Squires, K., A. L. Pozniak, G. Pierone, Jr., C. R. Steinhart, D. Berger, N. C. Bellos, S. L. Becker, M. Wulfsohn, M. D. Miller, J. J. Toole, D. F. Coakley, A. Cheng, and Study 907 Team.** 2003. Tenofovir disoproxil fumarate in nucleoside-resistant HIV-1 infection. Ann. Intern. Med. **139:**313–321.
31. **Srinivas, R. V., B. L. Robbins, M. C. Connelly, Y.-F. Gong, N. Bischofberger, and A. Fridland.** 1993. Metabolism and in vitro antiretroviral activities of bis(pivaloyloxymethyl) prodrugs of acyclic nucleoside phosphonates. Antimicrob. Agents Chemother. **37:**2247–2250.
32. **Starrett, J. E., Jr., D. R. Tortolani, J. Russell, M. J. M. Hitchcock, V. Whiterock, J. C. Martin, and M. M. Mansuri.** 1994. Synthesis, oral bioavailability determination, and in vitro evaluation of prodrugs of the antiviral agent 9-[2-(phosphonomethoxy)ethyl]adenine (PMEA). J. Med. Chem. **37:** 1857–1864.

33. **Tanaka, K., A. Yoshioka, S. Tanaka, and Y. Wataya.** 1984. An improved method for the quantitative determination of deoxyribonucleoside triphosphates in cell extracts. Anal. Biochem. **139:**35–41.
34. **Weislow, O. S., R. Kiser, D. L. Fine, J. Bader, R. H. Shoemaker, and M. R. Boyd.** 1989. New soluble-formazan assay for HIV-1 cytopathic effects: application to high-flux screening of synthetic and natural products for AIDS-antiviral activity. J. Natl. Cancer Inst. **81:**577–586.
35. **Yerly, S., T. V. Perneger, S. Vora, B. Hirschel, and L. Perrin.** 2000. Decay of cell-associated HIV-1 DNA correlates with residual replication in patients treated during acute HIV-1 infection. AIDS **14:**2805–2812.
36. **Zhang, H., G. Dornadula, M. Beumont, L. Livornese, Jr., B. Van Uitert, K. Henning, and R. J. Pomerantz.** 1998. Human immunodeficiency virus type 1 in the semen of men receiving highly active antiretroviral therapy. N. Engl. J. Med. **339:**1803–1809.